A Greenland ice core perspective on the dating of the Late Bronze Age Santorini eruption

Elin Löfroth

Examensarbete i geologi vid Lunds Universitet - Kvartärgeologi, no. 254
(45 hskp/ECTS)

Institutionen för geo- och ekosystemvetenskaper
Enheten för geologi
Lunds universitet
2010

A Greenland ice core perspective on the dating of the Late Bronze Age Santorini eruption

Master Thesis
Elin Löfroth

Department of Earth and Ecosystem Sciences
Division of Geology
Lund University
2010

Contents

Cover Picture: Santorini island, Greece - EOS photo NASA

A Greenland ice core perspective on the dating of the Late Bronze Age Santorini eruption

ELIN LÖFROTH

Löfroth, E., 2010: A Greenland ice core perspective on the dating of the Late Bronze Age Santorini eruption. E*xamensarbeten i geologi vid Lunds universitet*, Nr. 254, 22 pp. 45 ECTS credits.

Abstract: The Santorini eruption is one of the greatest in historic time and an important time marker in the regional archaeology. It has been dated to 1627-1600 BC (2σ error) using radiocarbon dating (Friedrich et al. 2006) and to 1642±5 BC by identifying a volcanic fallout layer in the Greenland ice cores (Vinther et al. 2006). However, archaeologists have estimated the eruption almost a century later than the other datings. The disagreement between the datings has caused a debate about the reliability of the different dating methods, with archaeologists questioning the radiocarbon and ice core datings as they do not agree within 2σ errors. Muscheler (2009) found that the discrepancy can also be seen when comparing records of cosmogenic radionuclides (^{10}Be and ^{14}C) in the GRIP ice core and IntCal04 tree ring data.

In this study a new ^{10}Be dataset from the NGRIP ice core is presented. It has a resolution of 7 years and spans the period 3752-3244 cal yr BP (1803-1295 BC). The NGRIP ^{10}Be record and the previously published ^{10}Be GRIP record were compared to IntCal datasets to investigate the discrepancy between the ice core and tree ring chronologies. By modelling the ^{14}C production rate based on atmospheric ^{14}C records a comparison could be made to the ^{10}Be flux which is assumed to represent the ^{10}Be production rate. This showed a time shift of ~23 years between the records. The sensitivity of the results to changes in important model parameters were evaluated. Uncertainties in the carbon cycle model may influence the inferred time shift in the order of 0-6 years.

The potential influences of climate and atmospheric processes on the ^{10}Be deposition were studied using δ^{18}O from the respective cores and GISP2 ice core ion data. The comparison to δ^{18}O revealed a negative correlation when the common production signal was removed from the ^{10}Be curves by subtracting the ^{14}C production rate curve. The ion data, as proxies for atmospheric circulation changes, did not show any correlations to the ^{10}Be record or the ^{10}Be/^{14}C difference.

When including possible data uncertainties there is still a minimum discrepancy of ~10 years between the ^{10}Be ice core and the ^{14}C tree ring record. Due to lack of alternative explanations it is concluded that the ice core and/or the tree ring chronologies contain unaccounted errors in this range.

Keywords: Santorini, ^{10}Be, ^{14}C, NGRIP, carbon cycle modeling.

Elin Löfroth, Department of Earth and Ecosystem Sciences, Division of Geology, GeoBiosphere Science Centre, Lund University, Sölvegatan 12, SE-223 62 Lund, Sweden. E-mail: elinlofroth@gmail.com

Ett Grönländskt isborrkärneperspektiv på dateringen av Santoriniutbrottet under sen bronsålder

ELIN LÖFROTH

Löfroth, E., 2010: A Greenland ice core perspective on the dating of the Late Bronze Age Santorini eruption. *Examensarbeten i geologi vid Lunds universitet*, Nr. 254, 22 sid. 45 hp.

Sammanfattning: Santoriniutbrottet är ett av de största under historisk tid och en viktig tidsmarkering inom den regionala arkeologin. Utbrottet har daterats till 1627-1600 år f.Kr. (2σ felmarginal) med ^{14}C-datering (Friedrich et al. 2006) och 1642±5 år f.Kr. genom identifiering av ett vulkaniskt lager i de Grönländska isborrkärnorna (Vinther et al. 2006). Arkeologer har dock uppskattat utbrottet till ungefär ett sekel senare än de andra dateringarna. Motsägelsen mellan dateringarna har orsakat en debatt om tillförlitligheten hos de olika metoderna, med arkeologer som ifrågasätter ^{14}C och isborrkärnedateringarna eftersom de inte stämmer överens inom 2σ-felmarginalen. Muscheler (2009) fann att diskrepansen även finns vid jämförelse av kosmogena radionuklider i GRIP isborrkärnan och i trädringsdata från IntCal04.

I den här studien presenteras ett nytt ^{10}Be-dataset från NGRIP isborrkärnan. Dataserien har en upplösning på 7 år och täcker perioden 3752-3244 BP (1803-1295 f.Kr.). Det nya datasetet från NGRIP och tidigare publicerade ^{10}Be data från GRIP jämfördes med IntCal-trädringsdataserier för att undersöka diskrepansen mellan trädrings– och isborrkärnekronologierna. Modellering av produktionshastigheten för ^{14}C grundat på ^{14}C data möjliggjorde jämföras med ^{10}Be fluxen som antas representera produktionshastigheten av ^{10}Be. Denna jämförelse visade på en tidsförskjutning mellan dataseten på runt 23 år. Resultatens känslighet för förändringar i viktiga parametrar i kolcykelmodellen utvärderades. Osäkerheter i modelleringen kan påverka den beräknade tidsförskjutningen med storleksordningen 0-6 år.

Den möjliga påverkan på depositionen av ^{10}Be från klimatet och atmosfäriska processer undersöktes med hjälp av δ^{18}O från båda isborrkärnorna samt jon-data från GISP2-isborrkärnan. Jämförelsen mellan ^{10}Be och δ^{18}O avslöjade en negativ korrelation då den gemensamma produktionssignalen mellan ^{14}C och ^{10}Be togs bort genom att subtrahera ^{14}C kurvan från ^{10}Be-data. Jon-data, som fungerar som en proxy för förändringar i den atmosfäriska cirkulationen, visade inga korrelationer med ^{10}Be eller differensen mellan ^{14}C och ^{10}Be.

När osäkerheterna från dataseten inkluderas finns fortfarande en diskrepans på minst 10 år mellan ^{10}Be från isborrkärnearkivet och ^{14}C från trädringsarkivet. I och med bristen på alternativa förklaringar dras slutledningen att isborrkärnekronologin och/eller trädringskronologin innehåller okända fel på runt 10 år.

Nyckelord: Santorini, ^{10}Be, ^{14}C, NGRIP, kolcykelmodellering

Elin Löfroth, Institutionen för geo- och ekosystemvetenskaper, Enheten för Geologi, Centrum för GeoBiosfärsvetenskap, Lunds Universitet, Sölvegatan 12, 223 62 Lund, Sverige. E-post: elinlofroth@gmail.com

1 Introduction

The dating of the Santorini eruption in the Late Bronze Age is still surrounded by uncertainties. The eruption is one of the greatest in historic time, with an approximated ejecta volume of over 100 km^3, and has been estimated to about ten times as explosive as Krakatau's eruption in 1883 (McCoy, 2009). Remains of the eruption can be found over large areas and the event is an important time marker in the regional archaeological chronology as it had a huge impact on the Minoan civilization. In order to determine the international relations of the Aegean region, especially to Egypt, it is important to know the timing of the eruption (Warren 2009).

The eruption has been dated to 1627-1600 BC (95.4% confidence interval) using radiocarbon dating of an olive branch buried by the eruption (Friedrich et al., 2006) and to 1642±5 BC by identifying a volcanic fallout layer and using annual layer counting in the Greenland ice cores (Vinther et al. 2006). The difference between the ^{14}C-dating and the ice core dating is only within the bounds of the methods uncertainty limits if the confidence interval is increased to 99.7% and because of this their reliability has been questioned. Furthermore, according to archaeological records based on links between the Minoan and Egyptian civilizations the eruption should have occurred 1550-1500 BC (Warren 1984, Wiener 2009). A summary of some published dates is shown in figure 1. These differences have spurred a debate about the timing of the eruption and the reliability of the respective methods, with natural scientists and some archaeologists supporting an earlier dating of the eruption and (other) archaeologists favouring the traditional archaeological dating (Warburton 2009).

In a geological perspective the difference in itself is of interest. The differences between the ^{14}C dating and ice core dating imply that the assumed errors are larger than currently believed if indeed the Santorini eruption is correctly identified in both records. A robust chronology is vital when studying geological processes. Dating allows us to find synchronised events in different parts of the world and hypothesise about possible causes. When working with systems that have a short response time, such as climate, it is of even greater importance to get exact relative dating in order to examine climate responses and feedback mechanisms. By comparing timescales inferred with different methods we can gain further knowledge and thus improve the accuracy of the dating.

Two records for which this can be done are the ice core ^{10}Be and the tree ring ^{14}C record. ^{10}Be and ^{14}C are both formed when cosmic rays interact with the atmosphere and by comparing their variations in tree rings and ice cores it is possible to evaluate discrepancies between the time scales. This link was used by

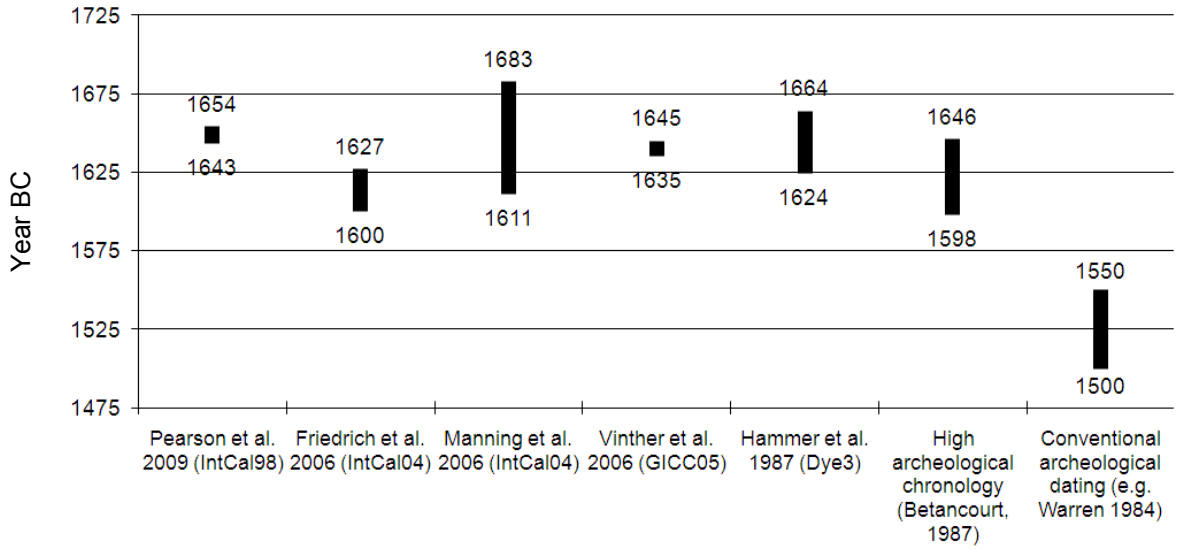

Fig. 1. Summary of some of the datings of the Santorini eruption. The datings are shown as black bars with 2σ errors for ^{14}C based records (Pearson et al., Friedrich et al. and Manning et al.), maximum counting errors for ice core records (Vinther et al. and Hammer et al.) and as archaeological estimates for archaeological records. The underlying chronology for the respective dates is given in brackets. The high archaeological chronology is a reinterpretation of archaeological data based on radiocarbon datings

Muscheler (2009) to evaluate the difference between the datings. From this comparison Muscheler found indications that there is an approximated 20 year difference between the two timescales around the time of the Santorini eruption. This supports the identification of the Santorini tephra in the ice core record but suggests that there are problems with tree ring chronology, ice core chronology, or both. Alternative explanations are uncertainties in the ^{10}Be transport and deposition, uncertainties or changes in the carbon cycle as well as problems in ^{14}C-data (Muscheler 2009).

In this thesis I will further investigate the difference between the timescales and what type of errors that may contribute to these. The focus will be on the suggested time shift between the ^{14}C and ^{10}Be curves 2000-1000 BC as a possible explanation for the dating discrepancy. Previously published records of ^{10}Be, tree -ring based IntCal calibration curves as well as new ^{10}Be data from the NGRIP (North GReenland Ice core Project) ice core will be used to compare the timing of production rate changes in ^{10}Be and ^{14}C data. The influence of climate on ^{10}Be deposition will also be discussed based on previously published δ^{18}O data from GRIP and NGRIP as well as GISP2 ion data.

Questions of interest:

- Is there a discrepancy between the ^{10}Be and ^{14}C records?
- Do the GRIP and NGRIP ^{10}Be curves show the same discrepancy to the ^{14}C calibration curve?
- Do the results change with different ways of calculating the ^{14}C production rate? How does this influence the discrepancy?
- How do climatic variations influence the deposition of ^{10}Be and can these variations influence the comparison between ^{10}Be and ^{14}C records?

2 Scientific background

The link between ^{10}Be and ^{14}C is very important for the subject of the study. The ^{10}Be and ^{14}C production, depositional processes as well as the atmospheric effects on ^{10}Be deposition are described in this section.

2.1 Production

Both ^{14}C (half-life 5730 years, Lal and Peters 1967) and ^{10}Be (half-life 1.5 My, Yiou and Raisbeck 1972) are produced in the atmosphere as galactic cosmic rays (GCR) reach the Earth (see figure 2). Primary GCR consist of protons (85%), alpha-particles (14%) and heavier nuclei (about 1%) and originate from outside our solar system (Lal and Peters 1967). When primary GCR interact with the atmosphere secondary particles are formed. These include muons, electrons and gamma rays. ^{10}Be is created by spallation; secondary cosmic ray particles hitting oxygen and nitrogen atoms causing nucleons to be emitted. The major production (~50-70%) of ^{10}Be occurs in the stratosphere but a relatively large part takes place in the troposphere (Lal and Peters 1967, Masarik and Beer 1999). The ratio depends on the altitude of the tropopause – at higher latitudes a smaller amount of ^{10}Be is produced in the troposphere. The ^{10}Be concentrations generally decrease closer to Earth because the production rate decreases and residence time is shorter (Feely et al. 1989). For ^{14}C, nitrogen capture of neutrons is responsible for over 99% of the production (Masarik and Beer 1999). Less energy is needed for the production of ^{14}C and thus in total less ^{10}Be is produced (Lal and Peters 1967). As a result, the direct response to solar particle emissions is also higher in ^{14}C production. A minor part of the production of both isotopes also occurs from solar ray particles, which have lower energies than the GCR.

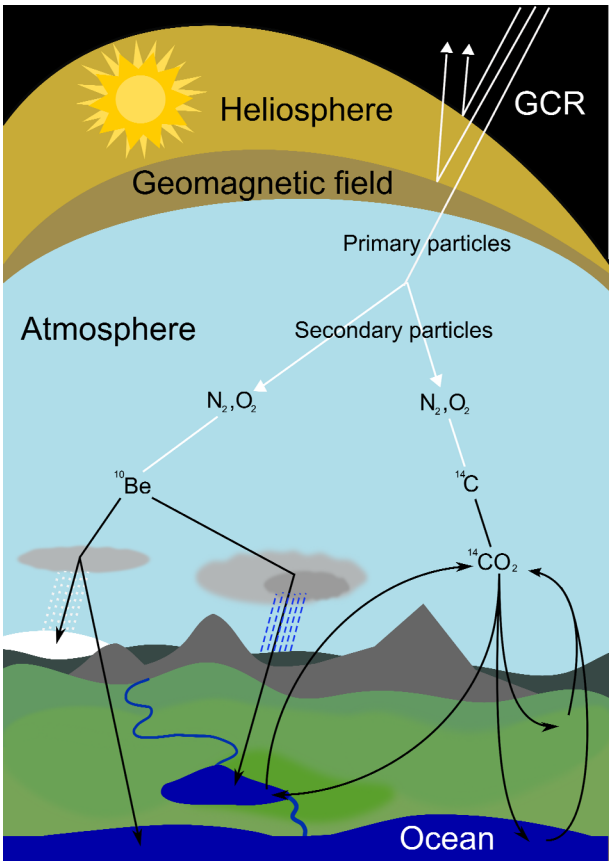

Fig. 2. Schematic summary of the production and deposition of ^{10}Be and ^{14}C. The white lines mark the steps in production and black lines mark depositional processes.

The influx of solar and cosmic ray particles determines the production rate of cosmogenic radionuclides. The Earth is protected from radiation by the solar magnetic field and the geomagnetic field, which deflect low-energy radiation. The influx of cosmic rays depends on the energy, charge and angle of incidence of the particles and the strength of the magnetic fields. The solar magnetic field varies with solar activity in periods of e.g. 11 years (the Schwabe cycle), 88 years (the Gleissberg cycle) and 207 years (the De Vries cycle) and are thus possible to study within a thousand year period. The strength of the geomagnetic field, on the other hand, varies over much longer timescales. The strength of the geomagnetic field is of great importance for the production rate at different latitudes since it deflects radiation more effectively at the magnetic equator.

The production of ^{10}Be and ^{14}C has been studied since the mid 20th century (e.g. Arnold and Al-Salih 1955, Libby 1946). Today the production process and the influence from solar activity and geomagnetic field changes are well understood. It is possible to test our understanding by comparing model results to experimental data and data from geological records. This has been done by e.g. Masarik and Beer (1999, 2009), who presented modelled results showing a good agreement with measured data.

2.2 Depositional processes

The depositional processes of ^{14}C and ^{10}Be differ, making it a very important fact to consider when interpreting such data from geological archives.

2.2.1 ^{14}C

After ^{14}C has been produced it forms CO_2 which follows the air masses to the lower troposphere and enters the carbon cycle. Through the carbon cycle ^{14}C becomes well mixed globally, which also dampens the production signal in the ^{14}C record.

Because of the suitable half-life, good mixing and the incorporation in organic materials radiocarbon is used for dating. Therefore ^{14}C and the influence of the carbon cycle has been well studied, e.g. through carbon cycle modelling. Through modelling it is possible to evaluate the effects of varying production rates and changes in the carbon cycle and to study production rate changes in the past. Carbon cycle models are also an important part of studying global warming and possible feedback mechanisms.

2.2.2 ^{10}Be

In contrast to ^{14}C, ^{10}Be attaches to aerosols and is transported with the air masses down to the lower troposphere where the aerosols are scavenged by droplets in clouds and deposited with precipitation or deposited directly. The atmospheric residence time of ^{10}Be formed in the stratosphere is about 1 to 2 years and a few weeks for tropospheric ^{10}Be (McHargue and Damon 1991).

The ^{10}Be signal in ice cores is more directly related to the production rate than ^{14}C found in tree rings, but as it is mixed in the atmosphere and deposited quite fast it might give a biased representation of the global production rate. The ^{10}Be record in ice cores is therefore more likely to be affected by weather and climate phenomena. Influences from these processes on the deposition might explain a part of the discrepancy between the ^{14}C and the ^{10}Be curves. So, how do atmospheric processes influence ^{10}Be deposition?

2.3 Atmospheric influence on ^{10}Be deposition

There is no general consensus concerning the atmospheric processes affecting the deposition of ^{10}Be. As ^{10}Be moves with the air masses it is dependant on atmospheric circulation patterns and changes in them. Concerning the exchange between the stratosphere and the troposphere some authors (e.g. Feely 1989) assign an important role to folding events in the upper troposphere, especially at mid-latitudes. Folding events are when the tropopause folds into the stratosphere. This allows flow of lower stratospheric air into the upper troposphere. For polar areas this would also mean that the influx of ^{10}Be-rich air is dependant on transport from mid-latitudes. Hence, the effects of periods of high exchange rates would be delayed at high latitudes. Holton et al. (1995), on the other hand, suggest that waves in the extratropical stratosphere drives the exchange, which occurs through a variety of processes at all latitudes.

Although the transport paths are not well known it is still possible to study the effects of intrusions of beryllium-rich air on the ^{10}Be record. Aldahan et al. (2008) showed that intrusions of beryllium-rich air masses can affect even annually averaged data, giving a skewed image of the production signal. Furthermore, such intrusions have been found to be suppressed at high latitudes when the polar vortex is stable (Baldwin and Dunkerton 2001). The polar vortex is a large scale cyclonic circulation pattern centred around each pole. Hence, if there are long periods of a very

stable polar vortex this might prevent mixing of air masses, resulting in an apparent drop in ^{10}Be concentration and vice versa.

Another important factor is precipitation variability, which could affect the concentration of ^{10}Be. Through modelling and comparisons to previous results Field et al. (2006) found that a warmer climate enhances precipitation over Greenland and thus dilutes the ^{10}Be concentration and that a colder climate could give an opposite effect. This is also seen in ^{10}Be from the Summit ice cores when comparing ^{10}Be concentrations from the Holocene to concentrations from the last glacial period (Wagner et al. 2001). Large volcanic eruptions, like Santorini, may also give a temporary cooling of the climate. Still, the influence on the ^{10}Be record would not be very great or long-lasting.

The sensitivity of ^{10}Be concentration to changes in precipitation motivate a correction for variations in the snow accumulation rate. This is done through calculating the ^{10}Be flux:

$$F = {}^{10}Be_{conc} * r_{acc} * \rho_{ice} \; [10^4 * \text{atoms/g ice}]$$

In this formula the flux (F) is multiplied by the rate of accumulation at the site (r_{acc}) and the density of ice (ρ_{ice}). However, as accumulation rate changes during the Holocene are relatively small it is not clear which of the concentration or the flux that provide the best representation of the global production rate during this period. As found by Horiuchi et al. (2006) ^{10}Be concentration at Dome Fuji shows greater similarities to the ^{14}C production rate than the ^{10}Be flux during some periods of the last 2000 years, indicating that it better represents the global production rate during these periods. ^{10}Be is also included in general circulation models (GCM). One example is the ECHAM5-HAM used by Heikkilä et al. (2008) to study how well the solar signal is reproduced in ^{10}Be concentrations and deposition fluxes on short time scales. This study showed that there was a good correlation to the solar signal for both the concentration and flux.

3 Methods and datasets

3.1 Preparation of NGRIP ice core samples

NGRIP ice core samples were taken from the freezer at the Centre for Ice and Climate, University of Copenhagen. The core was pre-cut into 55 cm segments at the coring site. Most samples (113 out of 141) available for this project were also pre-cut into segments with a cross section of 3 cm*5 cm. To complete the missing segments samples with a cross section of ~2 cm*4 cm were cut from the main NGRIP core in Copenhagen. A total of 141 samples were packed and shipped to Uppsala. The samples were prepared at the Geoscience Department at Uppsala University in collaboration with Ann-Marie Berggren, Ala Aldahan and Inger Påhlsson. The samples were analyzed at the Tandem Laboratory by Göran Possnert.

Each 55 cm segment represents about 3.5 years. Since the IntCal04 data has a resolution of 5 years during the studied period a lower resolution was considered satisfactory for the project. Therefore two samples were combined to give a resolution of ~7 years per combined sample. The samples were prepared in random order to avoid large gaps in the data should problems arise with a consecutive sequence of samples. In the following passages the procedures used when preparing the samples are described. In order to get good measurements from the Accelerator Mass Spectrometer (AMS) and avoid contamination between the samples it was very important that the equipment was cleaned between each sample, thus these procedures are included in the description.

The combined samples were cut into smaller pieces using a band saw in order to simplify the cleaning of the samples. Each piece was then rinsed in distilled water to remove contaminations, e.g. drilling fluid, and placed in plastic boxes with lids. Before the first usage the boxes were cleaned with washing fluid and tap water and then rinsed with 1 mol HCl and distilled and deionised water. The samples were weighed and 0.25 mg ^{9}Be carrier was added using a digital pipette. Carrier was needed for the AMS measurements to define the ^{10}Be/^{9}Be ratio in the sample so that the amount of ^{10}Be could be calculated. It has the advantage that loss of ^{10}Be in the later stages would not affect the ^{10}Be/^{9}Be ratio. The samples were melted by aid of a microwave oven. This was done in short periods so that the samples would not become hot and evaporate. For every eighth NGRIP sample a blank sample of about 1000 g distilled water was also prepared in order to identify potential contamination and to correct for the ^{10}Be levels for ^{10}Be contaminations during the preparation process and erroneous ^{10}Be counts in the AMS measurement. The boxes were rinsed thoroughly with distilled water after each sample.

The melted samples were moved to plastic water containers with attached silicone tubes, which were rinsed thoroughly with distilled water both before and after each sample was run through it. The silicone tubes were connected to cation exchange columns (Bio -Rad Poly-Prep® column, prefilled with AG® 50W-

X8 resin, 100-200 mesh hydrogen form 0.8*4cm) marked with sample names. As the samples ran through the columns the beryllium remained in the column and the waste water was discarded. Cation columns were not re-used.

To extract beryllium from the columns an extension quartz tube was placed on each column and 25ml of 4 mol HCl was added to the samples. The acid leached Be from the resin and it was retained with a plastic centrifuge tube. Afterwards 16 ml of NH_4 was added to each sample to raise the pH value of the solution so that beryllium-hydroxide could form. Each sample was sealed with a lid and shaken in order for it to be well mixed. The samples were then left for ~24 hours in order for precipitation of beryllium-hydroxide to occur.

The samples were centrifuged for 20 minutes in order for the precipitate to be concentrated at the bottom. The waste was then poured out. Distilled water was added and mixed with the samples. The mixtures were then moved to quartz tubes using disposable plastic pipettes. Extra water was used to make sure that the samples were completely transferred from the plastic centrifuge tubes. After each sample the centrifuge tubes were cleaned with washing fluid and tap water, rinsed with 1 mol HCl and then with distilled water. Pipettes were never reused. Before usage, the quartz tubes were cleaned using 4 mol HCl, dried at ~60°C over night to remove hygroscopic water and weighed so that the sample weight could be calculated.

The quartz tubes were centrifuged for 20 minutes to separate the precipitate from the water. After pouring out the waste water, distilled water was added to and mixed with the samples using disposable plastic spatulas. The quartz tubes were centrifuged and washed with water one more time. After this the samples were centrifuged again and the waste water poured out.

The quartz tubes were put in a furnace and dried for several hours at 60-80°C. After initial drying the temperature was increased to 150°C and kept at this temperature for two hours in order for the samples to become completely dry. Subsequently the temperature was raised to 850°C over a period of two hours and then kept this level for two more hours so that the samples could oxidise to beryllium oxide (BeO). The samples were allowed to cool to 110-150°C before they were moved to an desiccator to cool down.

The samples were weighed and Nb powder of 2 -3 times of the sample weight was added. The BeO was crushed and mixed with the Nb. About half of the mixture was used for pressing samples for AMS measurements. The rest of the samples were kept in storage as a backup until the AMS measurements were finished.

3.2 Previously published data

In order to study the observed discrepancy between ^{10}Be and ^{14}C data the new NGRIP ^{10}Be dataset is compared to several previously published datasets.

For the NGRIP ice core datings were available from the GICC05 timescale with a 20 year resolution on a depth scale published by Vinther et al. (2006). The δ^{18}O values from NGRIP were available at 20 year resolution on the GICC05 timescale. Both records are available from the Centre for Ice and Climate, University of Copenhagen.

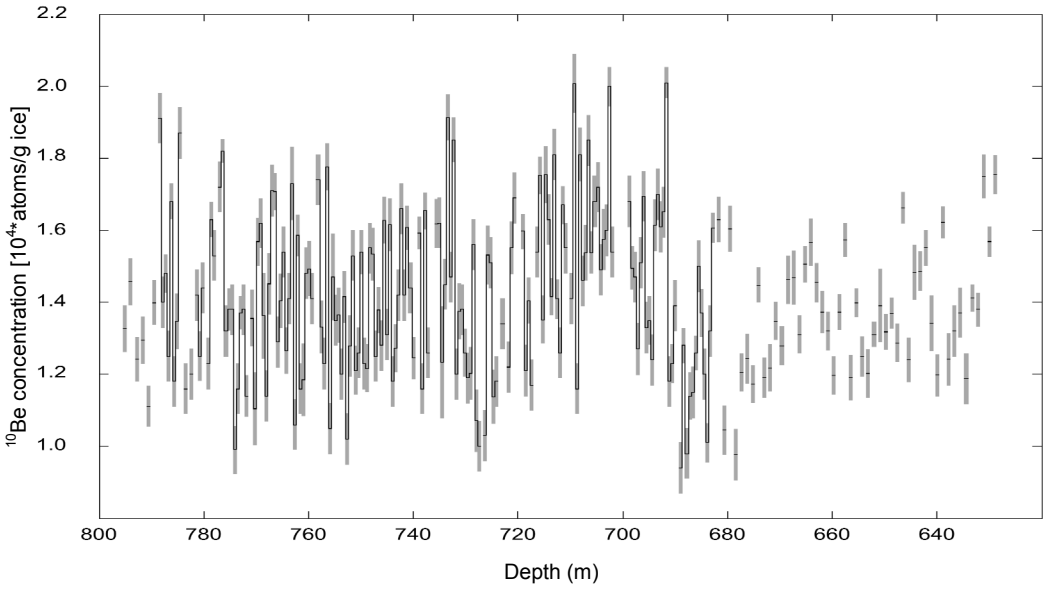

Fig. 3. GRIP ^{10}Be concentration (black line) on depth a scale with errors (grey area). The availability of ^{10}Be data points varies during the studied period (3950-2950 BP). Most notable are the missing data points between 628.65-682.55 m, representing the period 3265-2950 BP. Data from Muscheler et al. (2004).

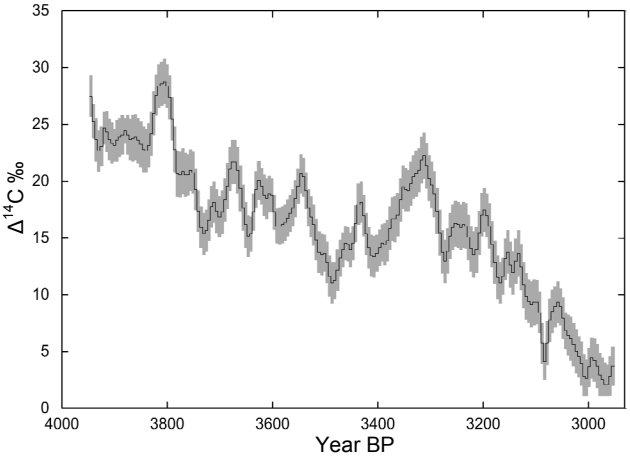

Fig. 4. IntCal04 $\Delta^{14}C$ [‰] marked in black with 1 σ errors marked in grey (Reimer et al. 2004) . $\Delta^{14}C$ shows the relative changes in ^{14}C compared to a standard.

The GRIP record of ^{10}Be, shown in figure 3, and $\delta^{18}O$ with a 3-4 year resolution were available from Muscheler at al. (2004) and Johnsen et al. (1997). The GRIP record is used as a complement to the NGRIP data as it encompasses the period 2000-1000 BC (3950-2950 BP). As seen in figure 3 there are some data points missing in the record, mainly after 3265 BP where every other data point is missing since these measurements have not been performed. There are also some data points missing in the period that the new NGRIP dataset encompasses.

For ^{14}C there are several records available. The ^{14}C measures in tree-rings is usually shown as $\Delta^{14}C$, which is the relative ^{14}C value compared to a standard and given in per mille. The Intcal04 calibration curve (Reimer et al. 2004) and two of the underlying datasets from The University of Washington (Stuiver et al. 1998b) and the Queen's University of Belfast (Pearson et al. 1986) were used (figure 4, 5a and 5b). The underlying datasets were used as a comparison to study if the time shift is present also for the original data and not only in the statistically treated IntCal04. The Washington and Belfast datasets were chosen because both encompass the period 3950-2950 BP. The former calibration curve, the IntCal98 curve (Stuiver et al. 1998), was also used for comparison (figure 5c). As seen in the figures the resolutions of the records vary somewhat. The IntCal04 has a resolution of 5 years, based on statistical treatment of the underlying datasets. The IntCal98 that has a resolution of 10 years. The Washington record has a resolution of 10 years and the Belfast record has a general resolution of 20 years.

To investigate the possible influences of climate and atmospheric processes ion data from the GISP2 ice core were used (Mayewski et al. 1997)

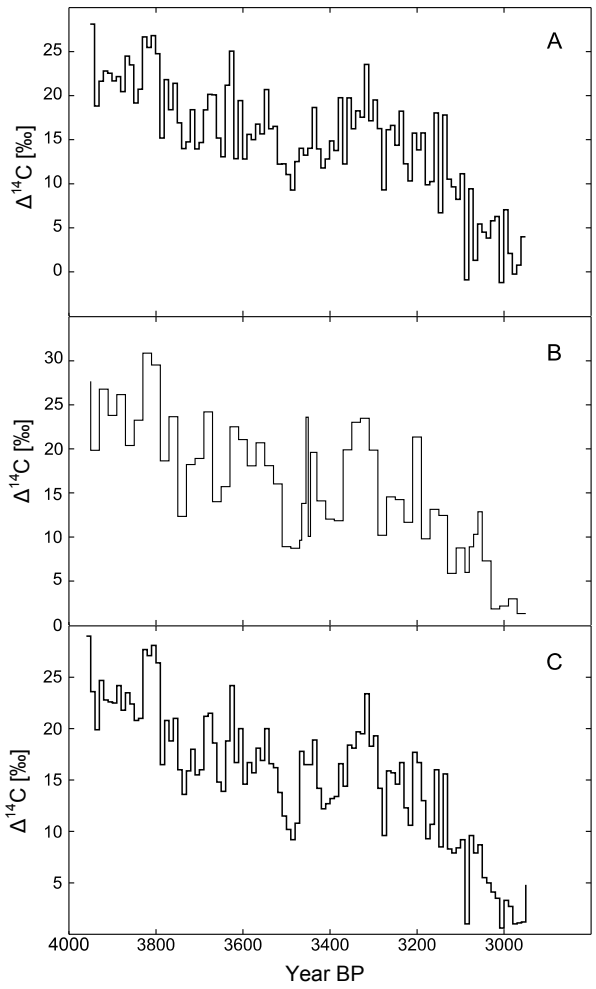

Fig. 5. Comparison of different $\Delta^{14}C$ [‰] records for the period 3950-2950 BP. The datasets shown are two sub-datasets of the IntCal04 from the University of Washington (A) (Stuiver et al. 1998b), the Queen's University of Belfast (B) (Pearson et al. 1986) and the previous calibration curve IntCal98 (C) (Stuiver et al. 1998).

3.3 Data analysis

The timing of the relative production changes in the datasets was compared through visual and statistical analysis. In order to compare datasets of different resolution all data were interpolated to an annual resolution. Because of the differences in production and depositional processes the ^{10}Be and ^{14}C data are not directly comparable. However, there are ways in which these differences can be addressed.

The different production processes give higher ^{14}C-production responses to solar particle emission changes. This was compensated for by multiplying the relative ^{10}Be changes around the mean by a factor of 1.3 (Masarik and Beer 1999, Muscheler 2000). The long term trends of the datasets over the studied period were removed to facilitate visual comparison of the datasets and to ensure that they do not affect later cal-

culated correlation coefficients. This was done through linear detrending.

3.3.1 Accumulation rates and ^{10}Be

As ice core ^{10}Be is deposited with precipitation, variations in the accumulation rate may influence the concentration. Compensating for accumulation variability can be done by calculating the ^{10}Be flux. The flux is calculated as the concentration multiplied by the density of ice and the accumulation rate. However, as mentioned previously it is not determined which of the concentration or the flux that is closest to the actual production rate. The flux was calculated for both the NGRIP data and the GRIP data. For the NGRIP ice core an estimated accumulation rate was calculated using depth and the GICC05 timescale (Vinther et al. 2006). The calculated accumulation rate was then detrended to compensate for compression effects. For GRIP the accumulation was also calculated using depth and the GICC05 timescale. The correction for ice flow effects used in the calculation was taken from Johnsen et al. (2001).

3.3.2 Carbon cycle modelling

An important step when comparing the ^{10}Be and ^{14}C data is compensating for the different depositional processes. The quick deposition of ^{10}Be makes it a more direct representation of its production rate whereas the ^{14}C enters the carbon cycle where it is mixed in the atmosphere, biosphere and the oceans. To compare the Δ^{14}C record with the ^{10}Be record the ^{14}C production rate is needed. By using a carbon cycle model a ^{14}C production rate can be modelled based on tree ring Δ^{14}C data. In doing this it is assumed that the carbon cycle during the studied period is well represented in the model. A comparison of the Δ ^{14}C (input) and the modelled ^{14}C production (output) is shown in figure 6. The modelled ^{14}C production rate can then be compared to the ^{10}Be production rate. The model used in this study was supplied by Raimund Muscheler. It is programmed in MatLab Simulink and based on Ulrich Siegenthaler's outcrop-diffusion model (1983). Further details are given in Muscheler et al. (2005). The model will hereafter be referred to as the box diffusion model.

As seen in the comparison of Δ ^{14}C and modelled ^{14}C production (figure 6) there is a shift in the amplitudes of the curves and a slight time shift between model input and output. Since the response to production changes is not direct in the atmospheric Δ ^{14}C record this is to be expected. However, since the timing is of importance in this study it is interesting to

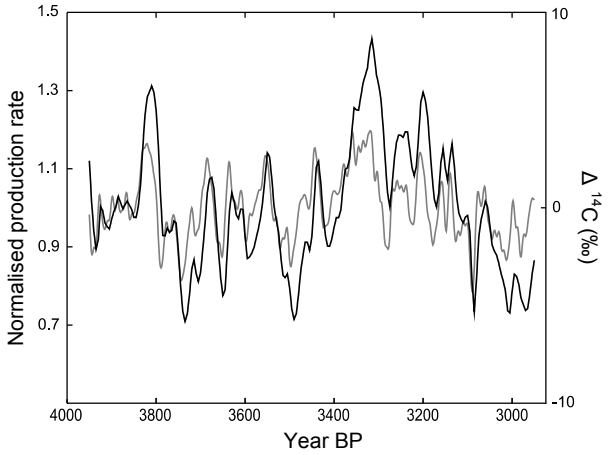

Fig. 6. Comparison of Δ ^{14}C, black curve, and the modeled ^{14}C production, grey curve. There is a slight difference in timing of the peaks. The main change is in the amplitudes of the curves. Note the different units on the y-axes.

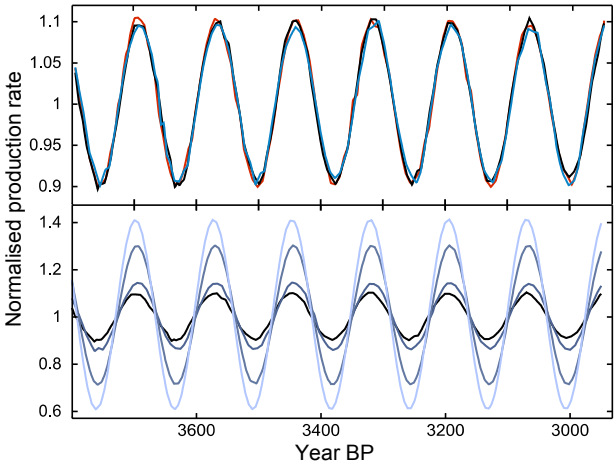

Fig. 7. Comparison of modelling outputs when varying parameter values. The top panel shows variation of the K parameter. The K values are 3005 (red curve), standard setting 4005 (black curve) and 5005 (blue curve). It is clear from this comparison that model results do not depend greatly on the K value since large changes in the parameter do not change the output to a large extent. The bottom panel shows variation of the a_c parameter. The diagram shows the standard setting of zero and increased values 0.01 (dark blue), 0.05 (blue) and 0.1 (light blue). It can be seen that increasing values for a_c yield higher amplitudes in the model output and 0-3 year changes in the timing of production rate peaks and troughs.

investigate if the model output is dependent on parameter values.

To test the model dependency of the results the modelling was redone several times with different values for two important model parameters. This was done to ensure that the results are not an artefact depending on modelling parameters. A comparison of the changes in model output with different model settings for a sine wave representing typical periodicities found in production data can be seen in figure 7. The parameters ad-

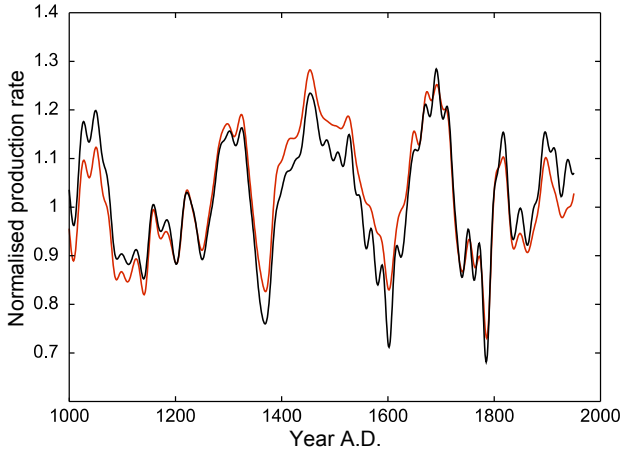

Fig. 8. Comparison between the box diffusion model (black curve) and the Bern3D model (red curve) (Müller et al. 2006). The main difference between the curves is the amplitudes of the peaks and troughs. Muscheler et al. (2007).

justed were the diffusion constant (K) and outcrop area (a_c). The diffusion constant determines the speed of which carbon can move between the ocean layers of the model. The outcrop area is the ocean surface area that is in contact with deep ocean layers and represents a model parameterization of deepwater formation (Siegenthaler 1983).

A further way of testing the reliability of the modelled ^{14}C production rate is to compare model performance to more recent models. This was done by Muscheler et al. (2007) who compared the box diffusion model to more recently developed models like the Bern3D model (Müller et al. 2006). The results from the comparison of the box diffusion model with standard settings to the Bern3D model are shown in figure 8. The comparison was also done with varied model parameters.

Based on the comparison of model output with varied parameter values we can expect that the amplitude of the modelled ^{14}C production will vary and that the timing of the peaks and depressions might vary slightly. The difference in the timing of the peaks in figure 7 is 1-3 years. The comparison to the Bern3D model clearly shows that the model performance is good in relation to more complex models. There is some variation in the amplitudes of the curve as well as in the timing of the peaks and troughs.

After modelling the ^{14}C production rate was compared to the ^{10}Be concentration and flux. Comparison of the timing of individual peaks in the ^{10}Be and ^{14}C datasets was first done visually and through measurements between chosen peaks and valleys. For a more objective analysis the correlations between the different datasets with and without time lags up to ±50 years were also calculated.

3.3.3 Atmospheric influences

Possible climatic influences on the ^{10}Be flux were studied by comparison with $\delta^{18}O$ from the respective cores. $\delta^{18}O$ is used in palaeoclimatology to infer climatic changes such as temperature and precipitation changes. To evaluate possible influences from atmospheric changes on Greenland around the time of the Santorini eruption ion concentration data from the GISP2 ice core were used.

A comparison was made to the ^{10}Be flux data as well as ^{10}Be flux after removing the long term trend in the flux calculated with a 4 degree polynomial. Also the ^{14}C curve was used as a representation of the common production signal and subtracted from the unfiltered ^{10}Be flux. This was done to focus the comparison on the short-term changes.

Correlation coefficients were calculated to investigate the common signals in the data and visual analysis was used for the comparison of the ^{10}Be flux with the ion data.

4 Results

4.1 ^{10}Be data

The new NGRIP ^{10}Be dataset (figure 9) covers a period from 3752 to 3244 years BP. It has a resolution of ~7 years. After the dataset was analysed, eight samples were re-analysed. This was done because two samples in the dataset appeared to have been mixed with blank samples. This could not resolve the problem and therefore these two data points were removed from the dataset for the following analysis. The results from the

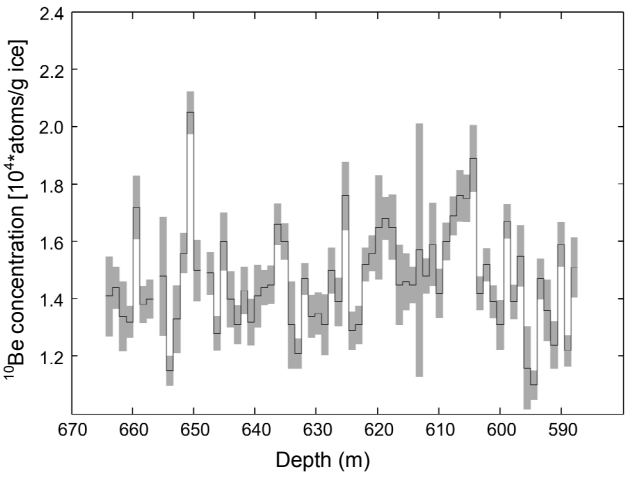

Fig. 9. Results of ^{10}Be measurements from NGRIP ice samples on a depth scale. The black line shows mean concentration values and the grey areas show the 1 σ error. The data covers the period between 3752 and 3244 years BP.

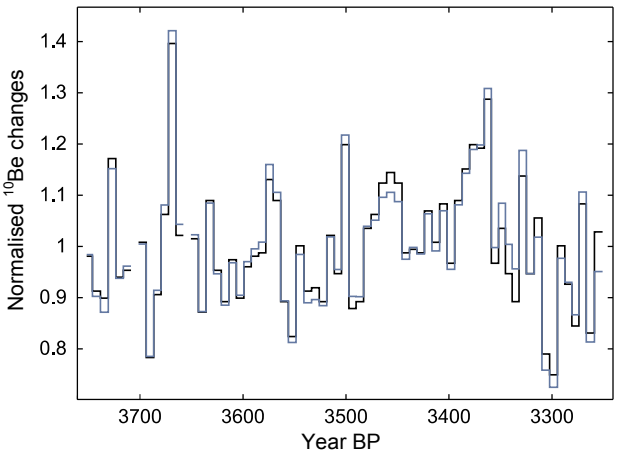

Fig. 10. Comparison of the NGRIP ^{10}Be concentration (black) and the calculated flux (blue). Differences between the data points are small and within the errors of the measured ^{10}Be concentration.

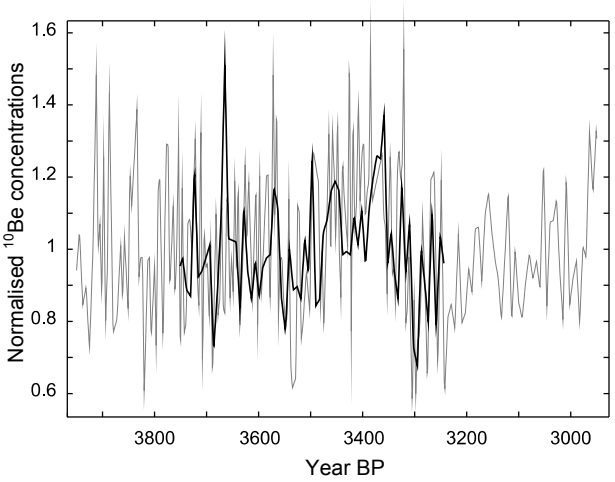

Fig. 11. Comparison of the normalised NGRIP ^{10}Be concentration (black) and the GRIP ^{10}Be concentration (grey) (Muscheler et al. 2004).The NGRIP data covers a shorter period than the GRIP data and has a lower resolution but show similar variations over the examined period.

re-measurements of the other samples were added to the dataset after calculating weighted means. A comparison between measured ^{10}Be concentrations and fluxes are shown in figure 10.

The calculated flux does not differ much from the concentration. Because of the stronger correlation with GRIP ^{10}Be and IntCal04 ^{14}C data, fluxes were used in later comparisons. A comparison between the NGRIP and GRIP ^{10}Be concentrations is shown in figure 11. The GRIP data has a higher resolution and greater variations than the NGRIP ^{10}Be flux. The same periods of high production can be found in both records. The only difference is the peak at 3665 year BP in the NGRIP data, which is given by one data point. The correlation coefficient of the two records is 0.48 for the concentrations and 0.57 for the fluxes (table 1). Both are significant at the 99.9% level.

4.2 Comparison between ^{10}Be and ^{14}C datasets

4.2.1 Visual analysis

Visual analysis involving calculation of offsets between peaks and valleys of the curves is not an objective way of studying the data, however it still gives some information about the time shift.

Figure 12 shows the NGRIP ^{10}Be flux and the ^{14}C production rate based on IntCal04 and calculation of offsets between some selected peaks and troughs. These were chosen because of their proximity to each other. Also, the production increase and decline between ~3400 to ~3300 appears to fit better when shifting the ^{10}Be curve towards younger ages. It is important to note that this does not necessarily show the actual time shift since it is not possible to know if the selected peaks and troughs represent the same production changes. The measurements in figure 12 do not give a consistent answer to how large the discrepancy between the curves is. The difference varies between

Datasets compared	**Lag (years)**	**Correlation coefficient**	**Significance**
GRIP & NGRIP ^{10}Be concentration (3752-3244 BP)	0	0.48	>99.9%
GRIP & NGRIP ^{10}Be flux (3752-3244 BP)	1	0.57	>99.9%
IntCal04 ^{14}C & NGRIP ^{10}Be concentration (3752-3244 BP)	26	0.45	>99.9%
IntCal04 ^{14}C & NGRIP ^{10}Be flux (3752-3244 BP)	25	0.52	>99.9%
IntCal04 ^{14}C & GRIP ^{10}Be concentration (3950-2950 BP)	18	0.32	>99.9%
IntCal04 ^{14}C & GRIP ^{10}Be flux (3950-2950 BP)	18	0.35	>99.9%
IntCal04 ^{14}C & GRIP ^{10}Be concentration (3752-3244 BP)	19	0.43	>99.9%
IntCal04 ^{14}C & GRIP ^{10}Be flux (3752-3244 BP)	20	0.52	>99.9%

Table 1. Correlation coefficients for the datasets compared for the time shifts with the highest correlation coefficients.

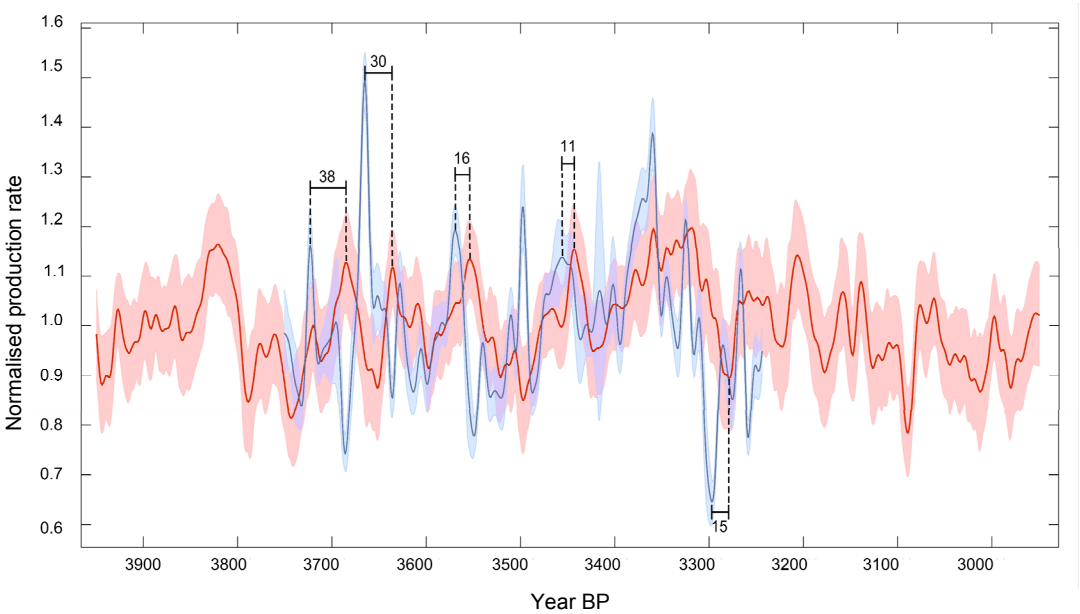

Fig. 12. The NGRIP ^{10}Be flux (blue line) with errors (light blue) and ^{14}C production rate (red line) with 1σ errors (pink). The NGRIP record has been low-pass filtered (20 yr) to remove noise. The ^{14}C production was calculated from low-pass filtered (10 yr) IntCal04 Δ^{14}C using 100 Monte Carlo runs. The numbers indicate the offset in years between some of the more pronounced peaks and troughs.

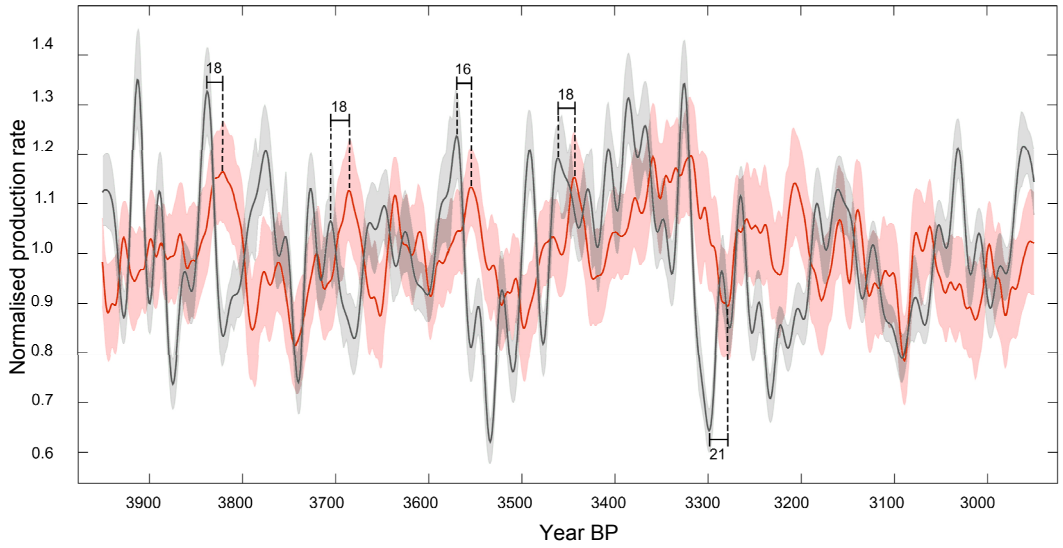

Fig. 13. The GRIP ^{10}Be flux (grey line) with errors (light grey) and ^{14}C production rate (red line) with 1σ errors (pink). The GRIP record has been low-pass filtered (20 yr) to remove noise. The ^{14}C production was calculated from low-pass filtered (10 yr) IntCal04 Δ^{14}C using 100 Monte Carlo runs. The numbers indicate the offset in years between some of the more pronounced peaks and troughs.

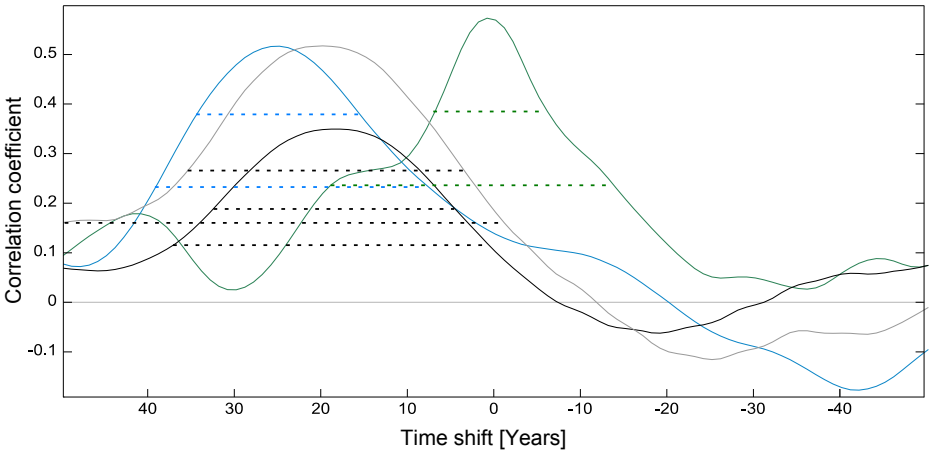

Fig. 14. The correlation coefficients with significances for different time shifts between NGRIP and GRIP ^{10}Be flux (green), NGRIP ^{10}Be flux and modeled IntCal04 ^{14}C production (blue), GRIP ^{10}Be flux and modeled IntCal04 ^{14}C production (black) as well as GRIP ^{10}Be flux 3752-3244 BP and modeled IntCal04 ^{14}C production (grey). The dashed lines in

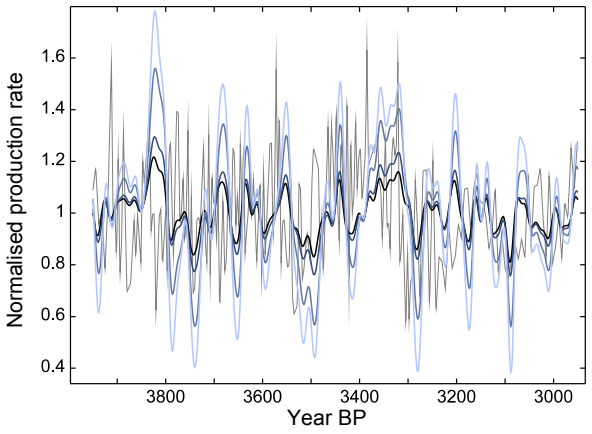

Fig. 15. Comparison of the GRIP ^{10}Be concentration (grey) to ^{14}C production rates modeled with different values for the a_c parameter. The ^{14}C production curves were low-pass filtered (20 yr) to facilitate the visual comparison of amplitudes.

38 and 11 years. The average difference based on these measurements is 22 years. The appearance of the peaks and troughs also differ between the records in terms of width and amplitude. This is also true for the IntCal04 comparison to the GRIP ^{10}Be flux (figure 13). For the GRIP dataset the measurements are more consistent with an age difference of around 18 years.

The measured discrepancies for both records both point to a difference of about 20 years. The agreement between the ^{10}Be and ^{14}C records vary in different periods of the time span, but a ~20 year shift of the ^{10}Be curves could improve the agreement for several of the peaks and dips.

4.2.2 Correlations

The correlation coefficients calculated with different lag times (±0-50 yrs) suggest a time shift of 18 years or more between the ^{10}Be datasets and the ^{14}C datasets. The highest correlation coefficients when comparing ^{10}Be flux to the modelled IntCal04 production rate were found with a lag between 18 and 25 years. The correlation coefficients with lag time are given in figure 14 and with significance in table 1.

However, for the modelled IntCal98 ^{14}C production the best correlation is found for lags between 19 and 27 years. For both comparisons the difference between the NGRIP and GRIP results decrease when correlations are calculated for the same period. The IntCal04 underlying datasets from University of Washington and Queen's University of Belfast also gave the best correlation when ^{10}Be was shifted to younger dates. The best fit was with a time shift between 30 and 31 years for dataset 1 and 27 to 43 years for dataset 2. It is notable that for all ^{14}C data series the correlation coefficients are higher when compared to ^{10}Be flux than when compared to ^{10}Be concentration.

Correlation coefficients gave similar results for different model values of *K*. For different model values of a_c the results differed concerning what offset to the ^{10}Be data gave the strongest correlation. The largest difference compared to the standard production rate result was six years. The correlation coefficients were higher for all a_c values larger than zero and highest for a_c=0.05. A comparison between the different production curves and GRIP ^{10}Be data is shown in figure 15.

4.2.3 Visual comparison with time shifts

Based on these correlations we can also do a visual analysis of the agreements when the ^{10}Be curves are shifted in time. The NGRIP curve was shifted 25 years (figure 16) and the GRIP curve was shifted 18 years (figure 17) as these time shift were suggested by correlation coefficients analysis. Several of the peaks and valleys show an improved agreement between the records when this is done. Also the larger scale variations like the peak between ~3400 and ~3300 seem to agree better for both records after applying these time

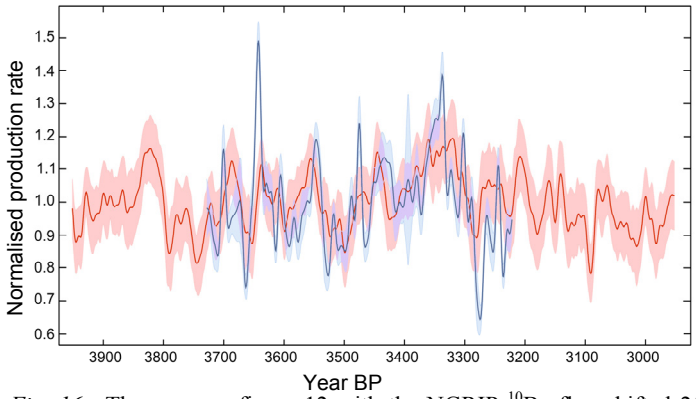

Fig. 16. The same as figure 12 with the NGRIP ^{10}Be flux shifted 25 years towards present day (to the right), as suggested by the calculated correlation coefficients.

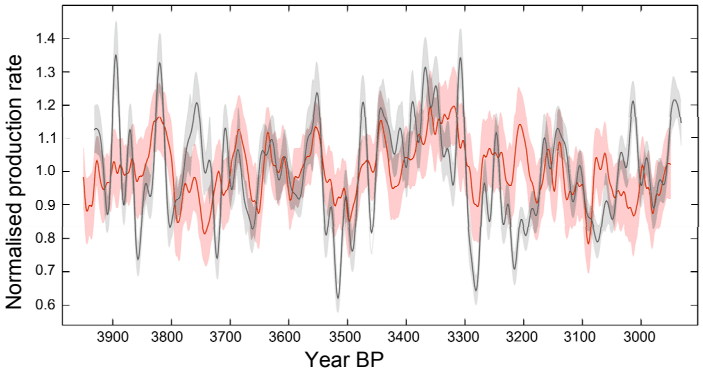

Fig. 17. The same as figure 13 with the GRIP ^{10}Be flux shifted 18 years towards present day (to the right), based on the highest correlation

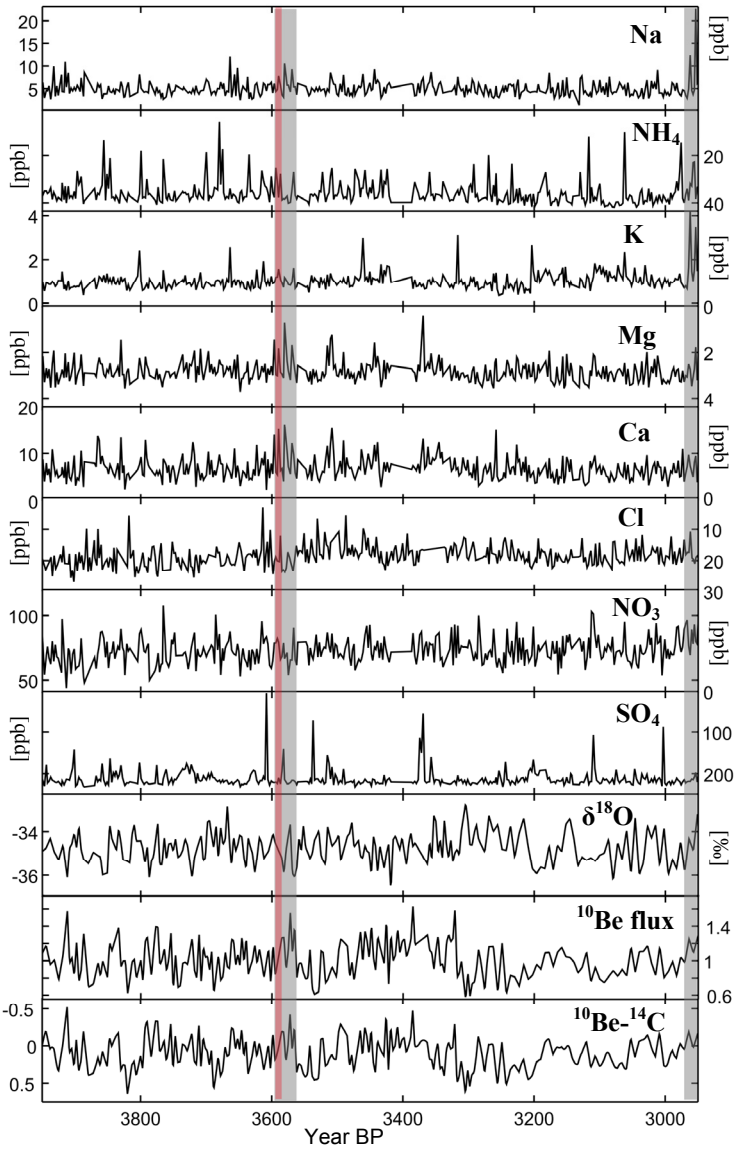

Fig. 18. Comparison of ^{10}Be records with proxies for atmospheric circulation changes and climate changes. From the top panels show concentrations of Na, NH_4, K, Mg, Ca, Cl, NO_3, SO_4, GRIP $\delta^{18}O$, normalised GRIP ^{10}Be flux and GRIP ^{10}Be flux minus the ^{14}C production rate curve (Johnsen et al. 1997, Mayewski et al. 1997, Muscheler et al. 2004). As the amplitudes in the ^{14}C production rate are less than in the ^{10}Be record the two curves have similar features. The red area marks the ice core dating of the Santorini eruption with the maximum counting error (Vinther et al. 2006). The grey areas show periods where peaks are seen in several of the ion records, as well as in the ^{10}Be GRIP data.

Datasets compared	Correlation coefficient	Significance
NGRIP ^{10}Be flux & δ18O (3752-3244 BP)	-0.05	-
Detrended NGRIP ^{10}Be flux & δ18O (3752-3244 BP)	-0.21	-
^{14}C-NGRIP ^{10}Be flux difference & $\delta^{18}O$ (3950-2950 BP)	-0.21	>99.9%
GRIP ^{10}Be flux & δ18O (3950-2950 BP)	-0.11	-
Detrended GRIP ^{10}Be flux & δ18O (3950-2950 BP)	-0.13	95%
^{14}C-NGRIP ^{10}Be flux difference & $\delta^{18}O$ (3950-2950 BP)	-0.14	>99.9%

Table 2. Correlation coefficients for the comparison between $\delta^{18}O$ and ^{10}Be flux and ^{10}Be flux with its long term trend removed.

shifts. There is also a peak between ~3200 and ~3100 that agrees better with these time shifts. There are still differences between the ^{10}Be and ^{14}C records after shifting the curves, but the timing of some individual peaks as well as the larger scale variations appear to agree better when time shifts are applied.

4.3 Atmospheric influences on deposition

The comparison between $\delta^{18}O$ and ^{10}Be fluxes show a negative correlation, as summarised in table 2. However, the correlation is relatively low compared to the comparison between ^{10}Be and ^{14}C and only significant for the GRIP data with the long term trend removed. When subtracting the ^{14}C production curve from the ^{10}Be fluxes, both the NGRIP and GRIP records show a negative correlation to $\delta^{18}O$. Table 2 shows a summary of the results.

The comparison between the GRIP ^{10}Be data and the ion concentration data is shown in figure 18. The GRIP record is used as it is available for a longer time period. There is no general agreement between the records, but some concentration peaks can be found in several records. At around 3600 BP there are increases in the concentrations of sodium, magnesium, calcium, chloride and sulphur. This also has a corresponding increase in the ^{10}Be flux and the ^{10}Be-^{14}C difference. Around this period, at 3608 and 3582 BP, we can also see two peaks in the SO_4 record. However, they are unlikely to be a reflection of the Santorini eruption as it has been dated to around 3590 BP. There is also an increase in several records at the end of the studied period. Both the sodium, ammonium and potassium show large peaks around 2950 BP. There is also an increase in the ^{10}Be and ^{10}Be-^{14}C difference after 3000 BP, but it is not larger than other peaks in the record. Some of the other ion records also show minor increases after 3000 BP. Correlation coefficients were also calculated between the ^{10}Be fluxes and each ion record. This gave no significant correlations.

5 Discussion

5.1 ^{10}Be uncertainties

The similarities between the new NGRIP ^{10}Be data and the previously published GRIP ^{10}Be data strengthen the reliability of the results. It has previously been found through principal component analysis (Beer et al. 2007) that 90% of the variance in the ^{10}Be GRIP record can be explained by the production signal. The main difference between the curves is the peak at 3665 year BP in the NGRIP data (figure 11). As this peak is based on one sample and not reflected in either the GRIP dataset or in the ^{14}C record it can be argued that it does not reflect a change in production rate. Concentration peaks could reflect low accumulation rates which could lead to higher concentrations of ^{10}Be. However, the peak does not change much when compensating for accumulation changes by calculating the ^{10}Be flux. The complete NGRIP data series can be considered reliable in terms of consistency with the GRIP ^{10}Be data. Still, possible mixing of samples lowers the credibility of individual measurements. Thus, this might be the explanation why the peak is not reflected in the other datasets.

The correlation coefficients of the NGRIP and GRIP data give a measure of their agreement. The slightly higher level of the correlation coefficients when comparing fluxes rather than concentrations might indicate that the fluxes are closer to the global production rate than the concentrations because of accumulation rate changes influencing the concentrations. This could also reflect a climate bias found in both records. Still, the correlation coefficients when comparing ^{10}Be and ^{14}C records are also higher for the fluxes which gives greater confidence to the flux as a reflection of the production signal. However, this only applies for the studied period. Which of the ^{10}Be flux and the ^{10}Be concentration that best reflects the production rate may vary for different periods, as found by e.g. Horiuchi et al. (2006).

Another consideration that should be made when interpreting the ^{10}Be data is the possibility of a polar bias in the ice core records. This could be caused by a higher local production response to changes in the solar magnetic field as the geomagnetic field is less effective in deflecting GCR at the poles. This would mean that the ice core ^{10}Be records discussed here might show higher production rate changes compared to the global production rate. Using ^{10}Be transport modeling with a general circulation model Field et al. (2006) found a polar enhancement of the solar-induced ^{10}Be production variations of about 1.2 compared to the global production rate. However, another modeling study by Heikkilä et al. (2009) found no indication of such a polar enhancement. The authors add that there may be a polar enhancement present that is lower than the noise level and therefore not seen in the results. Thus there might be a polar enhancement of the polar ^{10}Be response to solar magnetic field changes in the order of 1.2 or less.

5.2 ^{14}C uncertainties

The IntCal datasets are extensively used, as indicated by the many citations of the two articles (Stuvier at al. 1998: 2689 citations, Reimer et al, 2004: 1160 citations. Source: ISI Web of Knowledge 2019-01-10). However, the reliability of ^{14}C dating of the Santorini eruption has been questioned because of uncertainties in the method (Wiener 2009). His main arguments are that there is a problem when reproducing ^{14}C dating between different laboratories, that the errors of the measurements are too large to make the method useful in this context and that regional offsets to the calibration curve may give erroneous results.

The criticism offers an opportunity to investigate uncertainties in dating and improve the method. Kromer et al. (2001) have done this by examining possible effects from regional carbon offsets in the period around the Santorini eruption. One of the assumptions made in ^{14}C datings of terrestrial material is that ^{14}C is well equilibrated in each hemisphere, although it is not clear if this is true or not (Kromer et al. 2001 and references therein). Kromer and co-workers compared ^{14}C datings of absolutely dated tree ring records between Anatolia and Germany to investigate possible offsets. Their results showed that the offset existing is most likely due to differences in the growing season of the trees used for the comparison. Climate changes may also influence offsets in radiocarbon measurements through shifting of the growing season, thus adding uncertainty to interpretations (Chmielewski and Rotzer 2001, Kromer et al. 2001). During some periods there may be offsets resulting in dating differences in the order of 15-30 years. The possibility of regional offsets has been considered in the construction of the IntCal04 calibration curve, but as these are close to the precision of ^{14}C determinations and the offsets are likely to have varied over time they are difficult to estimate (Reimer et al. 2004).

5.3 The ^{10}Be and ^{14}C comparison

Local offsets between ^{14}C in Santorini and central Europe may have existed but since the Intcal04 calibration curve is absolutely dated even a minor systematic timescale shift compared to the ice core ^{10}Be records is unlikely. As ^{10}Be and ^{14}C productions are controlled by the influx of cosmic ray particles to the atmosphere but differ significantly in their depositional processes, the common signal in the records should be the production signal. The signal should also be simultaneous in the two records. Still, all records of ^{10}Be and ^{14}C compared here show that there is a difference in the timing of the ^{10}Be and the ^{14}C production curves. This is clear from both the visual analysis and the correlation analysis.

The GRIP ^{10}Be record was used to estimate the lag time over the 3950-2950 yr BP period as well as the period covered by the NGRIP data (table 1, figure 13, 17). The comparison for the common time period shows a closer agreement of the results regarding the timing of the ^{10}Be and ^{14}C variations (table 1). If NGRIP data for the 3950-2950 BP period were available the discrepancy for the highest correlation might change. Hence, it is more reasonable to use the same time periods to see if the NGRIP and GRIP records agree. It may be that NGRIP ^{10}Be for the entire period shows a time shift estimate closer to the GRIP estimate.

As shown in the correlation analysis, the 23 year discrepancy does not depend on the parameters of the box diffusion model. The time shift suggested by the correlation coefficients did vary (0-6 yr), especially with changes in the a_c parameter as it also did when comparing output values for the artificial curve (see figure 7). Hence, if the model would not accurately represent the actual operation of the carbon cycle for the studied period it could explain a systematic time shift between the datasets. The up to six years of difference can be regarded as the uncertainty of the model for this application. Nonetheless, even large modifications of the relevant model parameters do not lead to time shifts that are in the order of the discrepancy between the ^{10}Be and the ^{14}C records.

Interesting to note are the higher correlation coefficients between ^{10}Be flux and ^{14}C for the production rates calculated with higher values for the outcrop area, a_c. The production rate calculated with an a_c value of 0.05 gave the highest correlation. As shown in the methods (figure 7) the a_c parameter changes the amplitude of the variations in the output data. The amplitudes of the ^{10}Be and ^{14}C production rates differed when standard settings were used in calculating the ^{14}C production rate. When a higher value for a_c was used the amplitudes were increased, improving the correlation with the ^{10}Be data. Newer models, like the Bern3D model (Müller et al. 2006), include a parameter similar to the a_c in the carbon cycle model. As seen in the comparison by Muscheler et al. (2007), also shown in figure 8, the main difference between the modelled production rates are the amplitudes of the changes although these differences are not as great as produced when changing a_c alone. This result could suggest that the box diffusion model underestimates the exchange between the atmosphere and the deep ocean. However, the amplitudes of the ^{10}Be flux in the Greenland ice cores might be enhanced due to a polar enhancement and the Intcal04 curve could underestimate the amplitudes due to the applied smoothing of raw ^{14}C data. Thus the differences in amplitudes might result from the model, a potential polar enhancement of ^{10}Be response to solar magnetic field changes or the applied ^{14}C data.

The suggested time shifts differ more for different ^{14}C records than differently modelled ^{14}C production rates. This may depend on the resolution of the records, timing of the peaks and strong individual peaks. IntCal04 includes several improvements compared to the Intcal98 calibration curve. For the period 3950-2950 BP these improvements include a different statistical treatment of the underlying datasets to construct the curve and some additional data points from ^{14}C measurements on German oak trees, thus improving the reliability of the production rate modelled from Intcal04 Δ^{14}C. Furthermore, it combines data series from different regions, which should improve the reliability of the modelled production rate compared to the two underlying datasets. The individual records might contain regional offsets, influences from sampling methods, treatment of samples and other non-quantifiable errors (Reimer et al. 2004). Still, if one of the underlying datasets showed a much higher correlation or no time shift when compared to ^{10}Be flux it would be worth a further investigation. From the results we can conclude that this is not the case.

For the ^{10}Be data the residence time of ^{10}Be is important for the timing of peaks and troughs. Heikkilä et al. (2008) found that the residence times of ^{10}Be in the atmosphere may change as a result of changes in the amount of ^{10}Be produced in the stratosphere in relation to the troposphere. Changes in the atmospheric residence time of ^{10}Be would influence time shifts. However, to explain the time shift this would have to be in the order of 10 times the residence time,

which is not possible from changes in the ratio between stratospheric and tropospheric production.

When doing a cross correlation analysis it is important to consider potential biases. If strong peaks are present, agreements with these will influence the correlation coefficient more than agreement between smaller variations. It is also important to remember that there is a high correlation between the ^{10}Be and ^{14}C record also with slightly lower and slightly higher time shifts than for the maximum correlation. The significances of the correlation coefficients can be used as estimates of the error of the time shifts. For the comparison of the ^{10}Be flux and the IntCal04 ^{14}C production rate at the 99.9% limit give a time span of ~16-33 (see figure 14). Using the 95% limit the span is 8-38 years.

Therefore, based on the comparison between the ^{10}Be fluxes and the IntCal04 ^{14}C production rate it would be reasonable to estimate the time shift for 3752 -3244 BP to about 23 years with a uncertainty range of ~16-33 years. If we take into account the maximum error in the ice core chronology (±5 years) this leaves a discrepancy of ~18 years (11-28 years). Adding the modelling uncertainty based on the maximum difference (6 years) and the ^{10}Be residence time leaves us with a difference of ~10 years (3-21 years).

5.4 Atmospheric influence on ^{10}Be deposition

The comparison between the δ^{18}O and the ^{10}Be flux records show a negative correlation for the GRIP ^{10}Be record when comparing short-term variations (table 2). When removing the approximated solar signal by subtracting the ^{14}C production curve from the fluxes both records show a significant negative correlation to δ^{18}O. A negative correlation between δ^{18}O and ^{10}Be concentrations has been found on snowfall event scale by Pedro et al. (2006). This is suggested to depend on depletion in ^{10}Be in warm and moist air masses compared to cold air masses. They also concluded that this shows that the ^{10}Be record may be influenced by meteorological changes. This correlation has also been found on longer timescales in the GRIP ice core by Wagner et al. (2001). It is possible that the accumulation rate used to calculate the flux does not have the high resolution needed. Though, as the accumulation rate changes are not very big this would not explain the correlation. Thus, there seems to be climatic influences on the ^{10}Be concentration that cannot be removed by calculating the flux.

As seen in the comparison between the GRIP ^{10}Be flux and the ion data (figure 18) there are some similarities between the datasets. This may indicate that during some periods both records are sensitive to the same changes. The similarities could be produced by e.g. atmospheric circulation patterns. Atmospheric circulation patterns do effect the concentrations of ions in ice cores and could also change the transport patterns of ^{10}Be. The similarities found here can be compared to those of O'Brien et al. (1995) who studied common signals in the GISP2 ion data. They found several events during which the ion data indicated changes in the atmospheric circulation patterns in the polar area. A minor event ~3100-2400 BP was the only change mentioned around the time of the Santorini eruption. In this period marine species of the ions increased more than the non-sea salts, which was interpreted as a sign of a cooler climate (O'Brien et al. 1995) .

A cooler climate has been shown to result in higher ^{10}Be concentrations during the last glacial period (Wagner et al. 2001). In the comparison between the ion data and the GRIP ^{10}Be flux there is an increase in the concentrations of some of the ions after 3000 BP as well as in the ^{10}Be flux. As indicated by the ^{10}Be flux from which the ^{14}C production rate curve was subtracted this does not occur in the ^{14}C record. The concentration and flux in the GRIP record both show a similar trend in this period. Furthermore, even though there is a difference between the ^{10}Be and the ^{14}C record at this point in time the difference is not larger than at other times. Hence, according to the GISP ion record no large changes in atmospheric circulation patterns occurred during the Santorini eruption. There might be periods during which the ^{10}Be record is affected by climate changes, but at this time no such changes can be seen when comparing the ^{10}Be flux/^{14}C production rate difference to ion data.

Influences of climate and atmospheric processes on the ^{10}Be concentration and flux (as a measure for the production rate) has been examined by several authors. Beer et al. (2007) conclude that systematic effects on the ^{10}Be deposition account for about 10% of the variability in the GRIP record. According to Usoskin et al. (2006) the local climate is important for the ^{10}Be variations on time scales <100 years but the solar signal is still an important influence on these time scales. From GCM modeling it has been concluded that the solar signal is highly correlated to ^{10}Be flux variations in ice cores also on shorter timescales (1986-1990) (Heikkilä et al. 2008).

In summary, there are climatic and

atmospheric processes that influence ^{10}Be records, adding some uncertainty to production rate reconstructions. Based on the results and the discussion above there are atmospheric and climatic influences that must be taken into account when interpreting ^{10}Be ice core data. However, climatic and atmospheric effects on the ^{10}Be data show do not appear to cause systematic shifts in the ^{10}Be fluxes peaks and troughs on periods over 100 years.

5.5 Synthesis and outlook

The date of the Santorini eruption has been widely discussed (e.g. Betancourt 1987, Cadogan 1978, Friedrich et al. 2006, Manning et al. 2006, Pearce et al. 2004, Pearson et al. 2009, Siklosy et al. 2009, Warburton 2007). Several types of records have been used, each with their own challenges. The results presented here provide a possible explanation for the discrepancy between the ^{14}C datings and the ice core chronology.

As discussed above there are several uncertainties in the records that may affect the comparison. There is a climatic influence on the ^{10}Be deposition that influences the ^{10}Be concentration and flux. There are uncertainties regarding how well ice core ^{10}Be flux and modelled ^{14}C production rate represents the global production rates. These uncertainties may influence the comparison during certain periods, somewhat shifting the peaks. None of the uncertainties found are, however, likely to give systematic shifts in the timescale. The comparison between the ^{10}Be and ^{14}C records show a ~23 year discrepancy. Removing ice core counting errors, carbon cycle uncertainties and the residence time of ^{10}Be leaves a ~10 year difference of unaccounted errors. As the uncertainties discussed cannot explain the discrepancy the most likely explanation seems to be a shift between the ice core and the tree ring chronologies. This would reconcile some of the previously published datings, strengthening their reliability. As methodology improves in future research hopefully it will be possible to reach consensus about the date of the Santorini eruption and to solve the discrepancy between the tree ring and ice core records.

6 Conclusions

- There is a discrepancy between the ^{14}C tree ring record and the ^{10}Be ice core record of about 23 years.
- Both NGRIP and GRIP ^{10}Be data show discrepancies to the IntCal04 ^{14}C record.
- A part of the discrepancy (up to 6 years) may be explained by uncertainties when modelling the ^{14}C production rate.
- There is a climatic influence on the ^{10}Be data that cannot be removed by calculating ^{10}Be fluxes. This influences the comparison between ^{14}C and ^{10}Be but is unlikely to cause a systematic shift between the records.
- When summing up the uncertainties of the datasets and the method applied there is still a minimum 10 year discrepancy between the ^{10}Be ice core record and the ^{14}C tree ring record.
- This may indicate that there is a time shift between the chronologies, but also reconciles the ice core and tree ring datings of the Santorini eruption.

7 Acknowledgements

I would like to thank my supervisor Raimund Muscheler for all the help during this project. I also want to thank Ann-Marie Berggren for instructing me in the preparations of the ^{10}Be samples, Inger Påhlsson who helped with pressing the samples and Göran Possnert for doing the analyses.

8 References

Aldahan, A., Hedfors, J., Possnert, G., Kulan, A., Berggren, A.M., & Soderstrom, C., 2008: Atmospheric impact on beryllium isotopes as solar activity proxy. *Geophysical Research Letters 35*, L21812.

Arnold, J.R., & Al-Salih, H.A., 1955: Beryllium-7 produced by cosmic rays. *Science 121*, 451-453.

Baldwin, M.P., & Dunkerton, T.J., 2001: Stratospheric harbingers of anomalous weather regimes. *Science 294*, 581-584.

Beer, J., McCracken, K.G., Häilikkä, U., & Steinhilber, F., 2007: Long-term changes in cosmic rays derived from cosmogenic radionuclides. *In* Caballero, R., D'Olivo, J.C., Medina-Tanco, G., Nellen, L., Sánchez, F.A., & Valdés-Galicia, J.F., eds.) 30th International Cosmic Ray Conference, Volume 1: Mérida, Mexico, 765-768.

Feely, H.W., Larsen, R.J., & Sanderson, C.G., 1989: Factors that cause seasonal variations in beryllium-7 concentrations in surface air. *Journal of Environmental Radioactivity 9*, 223-249.

Field, C.V., Schmidt, G.A., Koch, D., & Salyk, C., 2006: Modeling production and climate-related impacts on Be-10 concentration in ice cores. *Journal of Geophysical Research-Atmospheres 111*, D15107.

Friedrich, W.L., Kromer, B., Friedrich, M., Heinemeier, J., Pfeiffer, T., & Talamo, S., 2006: Santorini eruption radiocarbon dated to 1627-1600 BC. *Science 312*, 548-548.

Heikkilä, U., Beer, J., & Feichter, J., 2009: Meridional transport and deposition of atmospheric Be-10. *Atmospheric Chemistry and Physics 9*, 515-527.

Heikkilä, U., Beer, J., Jouzel, J., Feichter, J., & Kubik, P., 2008: Be-10 measured in a GRIP snow pit and modeled using the ECHAM5-HAM general circulation model. *Geophysical Research Letters 35*, L05817

Holton, J.R., Haynes, P.H., McIntyre, M.E., Douglass, A.R., Rood, R.B., & Pfister, L., 1995: Stratosphere-troposphere exchange. *Reviews of Geophysics 33*, 403-439.

Horiuchi, K., Uchida, T., Sakamoto, Y., Ohta, A., Matsuzaki, H., Shibata, Y., & Motoyama, H., 2006: Ice core record of Be-10 over the past millennium from Dome Fuji, Antarctica: A new proxy record of past solar activity and a powerful tool for stratigraphic dating) Symposium of Accelerator-Based Mass Spectrometry: Tokyo, Japan, 253-261.

Johnsen, S.J., Clausen, H.B., Dansgaard, W., Gundestrup, N.S., Hammer, C.U., Andersen, U., Andersen, K.K., Hvidberg, C.S., Dahl-Jensen, D., Steffensen, J.P., Shoji, H., Sveinbjornsdottir, A.E., White, J., Jouzel, J., & Fisher, D., 1997: The delta O-18 record along the Greenland Ice Core Project deep ice core and the problem of possible Eemian climatic instability. *Journal of Geophysical Research-Oceans 102*, 26397-26410.

Johnsen, S.J., Dahl-Jensen, D., Gundestrup, N., Steffensen, J.P., Clausen, H.B., Miller, H., Masson-Delmotte, V., Sveinbjornsdottir, A.E., & White, J., 2001: Oxygen isotope and palaeotemperature records from six Greenland ice-core stations: Camp Century, Dye-3, GRIP, GISP2, Renland and North-GRIP. *Journal of Quaternary Science 16*, 299 -307.

Kromer, B., Manning, S.W., Kuniholm, P.I., Newton, M.W., Spurk, M., & Levin, I., 2001: Regional (CO2)-C-14 offsets in the troposphere: Magnitude, mechanisms, and consequences. *Science 294*, 2529-2532.

Lal, D., & Peters, B., 1967: Cosmic ray produced radioactivity on the Earth. In Flügge, S., (ed.): *Handbuch der Physik*. Springer, Berlin, 551-612.

Libby, W.F., 1946: Atmospheric Helium Three and Radiocarbon from Cosmic Radiation. *Physical Review 69*, 671.

Masarik, J., & Beer, J., 1999: Simulation of particle fluxes and cosmogenic nuclide production in the Earth's atmosphere. *Journal of Geophysical Research-Atmospheres 104*, 12099-12111.

Masarik, J., & Beer, J., , 2009: An updated simulation of particle fluxes and cosmogenic nuclide production in the Earth's atmosphere. *Journal of Geophysical Research-Atmospheres 114*, D11103.

Mayewski, P.A., Meeker, L.D., Twickler, M.S., Whitlow, S., Yang, Q.Z., Lyons, W.B., & Prentice, M., 1997: Major features and forcing of high-latitude northern hemisphere atmospheric circulation using a 110,000-year-long glaciochemical series. *Journal of Geophysical Research-Oceans 102*, 26345-26366.

McCoy, F.W., 2009: The eruption within the debate about the date. In Warburton, D.A., (ed.): Time's Up! Dating the Minoan Eruption of Santorini: acts of the Minoan Eruption Chronology Workshop, Sandbjerg November 2007: *Monographs of the Danish Institute at Athens*. The Danish Institute at Athens, Athens, 73-90.

McHargue, L.R., & Damon, P.E., 1991: The global beryllium 10 cycle. *Reviews of Geophysics 29*, 141-158.

Müller, S.A., Joos, F., Edwards, N.R., & Stocker, T.F., 2006: Water mass distribution and ventilation time scales in a cost-efficient, three-dimensional ocean model. *Journal of Climate 19*, 5479-5499.

Muscheler, R., 2000: Nachweis von Änderungen im Kohlenstoffkreislauf durch Vergleich der Radionuklide ^{10}Be, ^{36}Cl und ^{14}C. PhD Thesis. Naturwissenschaften ETH Zürich, Nr. 13941. 170 pp.

Muscheler, 2009: ^{14}C and ^{10}Be around 1650 cal BC. *In* Warburton, D.A., (ed.): Time's Up! Dating the Minoan Eruption of Santorini: acts of the Minoan Eruption Chronology Workshop, Sandbjerg November 2007: *Monographs of the Danish Institute at Athens*. Aarhus University Press, Aarhus, 273-282.

Muscheler, R., Beer, J., Wagner, G., Laj, C., Kissel, C., Raisbeck, G.M., Yiou, F., & Kubik, P.W., 2004: Changes in the carbon cycle during the last deglaciation as indicated by the comparison of ^{10}Be and ^{14}C records. *Earth and Planetary Science Letters 219*, 325-340.

Muscheler, R., Beer, J., Kubik, P.W., & Synal, H.A., 2005: Geomagnetic field intensity during the last 60,000 years based on Be-10 and Cl-36 from the Summit ice cores and C-14. *Quaternary Science Reviews 24*, 1849-1860.

Muscheler, R., Joos, F., Beer, J., Müller, S.A., Vonmoos, M., & Snowball, I., 2007: Solar activity during the last 1000 yr inferred from radionuclide records. *Quaternary Science Reviews 26*, 82-97.

O'Brien, S.R., Mayewski, P.A., Meeker, L.D., Meese, D.A., Twickler, M.S., & Whitlow, S.I., 1995: Complexity of Holocene Climate as Reconstructed from a Greenland Ice Core. *Science 270*, 1962-1964.

Pearson, C.L., Dale, D.S., Brewer, P.W., Kuniholm, P.I., Lipton, J., & Manning, S.W., 2009: Dendrochemical analysis of a tree-ring growth anomaly associated with the Late Bronze Age eruption of Thera. *Journal of Archaeological Science 36*, 1206-1214.

Pedro, J., van Ommen, T., Curran, M., Morgan, V., Smith, A., & McMorrow, A., 2006: Evidence for climate modulation of the Be-10 solar activity proxy. *Journal of Geophysical Research-Atmospheres 111*, D21105.

Rasmussen, S.O., Vinther, B.M., Clausen, H.B., & Andersen, K.K., 2007: Early Holocene climate oscillations recorded in three Greenland ice cores. *Quaternary Science Reviews 26*, 1907-1914.

Reimer, P.J., Baillie, M.G.L., Bard, E., Bayliss, A., Beck, J.W., Bertrand, C.J.H., Blackwell, P.G., Buck, C.E., Burr, G.S., Cutler, K.B., Damon, P.E., Edwards, R.L., Fairbanks, R.G., Friedrich, M., Guilderson, T.P., Hogg, A.G., Hughen, K.A., Kromer, B., McCormac, G., Manning, S., Ramsey, C.B., Reimer, R.W., Remmele, S., Southon, J.R., Stuiver, M., Talamo, S., Taylor, F.W., van der Plicht, J., & Weyhenmeyer, C.E., 2004: IntCal04 terrestrial radiocarbon age calibration, 0-26 cal kyr BP. *Radiocarbon 46*, 1029-1058.

Siegenthaler, U., 1983: Uptake of excess CO_2 by an outcrop-diffusion model of the Ocean. *Journal of Geophysical Research-Oceans and Atmospheres 88*, 3599-3608.

Stuiver, M., Reimer, P.J., Bard, E., Beck, J.W., Burr, G.S., Hughen, K.A., Kromer, B., McCormac, G., Van der Plicht, J., & Spurk, M., 1998: INTCAL98 radiocarbon age calibration, 24,000-0 cal BP. *Radiocarbon 40*, 1041-1083.

Usoskin, I.G., Solanki, S.K., Kovaltsov, G.A., Beer, J., & Kromer, B., 2006: Solar proton events in cosmogenic isotope data. *Geophysical Research Letters 33*, L08107

Wagner, G., Laj, C., Beer, J., Kissel, C., Muscheler, R., Masarik, J., & Synal, H.A., 2001: Reconstruction of the paleoaccumulation rate of central Greenland during the last 75 kyr using the cosmogenic radionuclides Cl-36 and Be-10 and geomagnetic field intensity data. *Earth and Planetary Science Letters 193*, 515-521.

Warburton, D.A., 2009: Epilouge. *In* Warburton, D.A., (ed.): Time's Up! Dating the Minoan Eruption of Santorini: acts of the Minoan Eruption Chronology Workshop, Sandbjerg November 2007: *Monographs of the Danish Institute at Athens*. Aarhus University Press, Aarhus, 293-298.

Warren, P., 1984: Archaeology - absolute dating of the Bronze-Age eruption of Thera (Santorini). *Nature 308*, 492-493.

Warren, 2009: The date of the Late Bronze Age eruption of Santorini. *In* Warburton, D.A., (ed.): Time's Up! Dating the Minoan Eruption of Santorini: acts of the Minoan Eruption Chronology Workshop, Sandbjerg November 2007: *Monographs of the Danish Institute at Athens*. Aarhus University Press, Aarhus, 181-186.

Wiener, M.H., 2009: The state of the debate. *In* Warburton, D.A., (ed.): Time's Up! Dating the Minoan Eruption of Santorini: acts of the Minoan Eruption Chronology Workshop, Sandbjerg November 2007: *Monographs of the Danish Institute at Athens*. Aarhus University Press, Aarhus, 197-206.

Vinther, B.M., Clausen, H.B., Johnsen, S.J., Rasmussen, S.O., Andersen, K.K., Buchardt, S.L., Dahl-Jensen, D., Seierstad, I.K., Siggaard-Andersen, M.L., Steffensen, J.P., Svensson, A., Olsen, J., & Heinemeier, J., 2006: A synchronized dating of three Greenland ice cores throughout the Holocene. *Journal of Geophysical Research-Atmospheres 111*, 11.

Yiou, F., & Raisbeck, G.M., 1972: Half-Life of ^{10}Be. *Physical Review Letters 29*, 372.

Tidigare skrifter i serien ”Examensarbeten i Geologi vid Lunds Universitet”:

205. Bergelin, Ingemar, 2006: $^{40}Ar/^{39}Ar$ geochronology of basalts in Scania, S Sweden: evidence for two pulses at 191-178 Ma and 110 Ma, and their relation to the break-up of Pangea.
206. Edvarssson, Johannes, 2006: Dendrokronologisk undersökning av tallbestånds etablering, tillväxtdynamik och degenerering orsakat av klimatrelaterade hydrologiska variationer på Viss mosse och Åbuamossen, Skåne, södra Sverige, 7300-3200 cal. BP.
207. Stenfeldt, Fredrik, 2006: Litostratigrafiska studier av en platåformad sand- och grusavlagring i Skuremåla, Blekinge.
208. Dahlenborg, Lars, 2007: A Rock Magnetic Study of the Åkerberg Gold Deposit, Northern Sweden.
209. Olsson, Johan, 2007: Två svekofenniska graniter i Bottniska bassängen; utbredning, U-Pb zirkondatering och test av olika abrasionstekniker.
210. Erlandsson, Maria, 2007: Den geologiska utvecklingen av västra Hamrångesynklinalens suprakrustalbergarter, centrala Sverige.
211. Nilsson, Pernilla, 2007: Kvidingedeltat – bildningsprocesser och arkitektonisk uppbyggnadsmodell av ett glacifluvialt Gilbertdelta.
212. Ellingsgaard, Óluva, 2007: Evaluation of wireline well logs from the borehole Kyrkheddinge-4 by comparsion to measured core data.
213. Åkerman, Jonas, 2007. Borrkärnekartering av en Zn-Ag-Pb-mineralisering vid Stenbrånet, Västerbotten.
214. Kurlovich, Dzmitry, 2007: The Polotsk-Kurzeme and the Småland-Blekinge Deformation Zones of the East European Craton: geomorphology, architecture of the sedimentary cover and the crystalline basement.
215. Mikkelsen, Angelica, 2007: Relationer mellan grundvattenmagasin och geologiska strukturer i samband med tunnelborrning genom Hallandsås, Skåne.
216. Trondman, Anna-Kari, 2007: Stratigraphic studies of a Holocene sequence from Taniente Palet bog, Isla de los Estados, South America.
217. Månsson, Carl-Henrik & Siikanen, Jonas, 2007: Measuring techniques of Induced Polarization regarding data quality with an application on a test-site in Aarhus, Denmark and the tunnel construction at the Hallandsås Horst, Sweden.
218. Ohlsson, Erika, 2007: Classification of stony meteorites from north-west Africa and the Dhofar desert region in Oman.
219. Åkesson, Maria, 2008: Mud volcanoes - a review. (15 hskp)
220. Randsalu, Linda, 2008: Holocene relative sea-level changes in the Tasiusaq area, southern Greenland, with focus on the Ta1 and Ta3 basins. (30 hskp)
221. Fredh, Daniel, 2008: Holocene relative sea-level changes in the Tasiusaq area, southern Greenland, with focus on the Ta4 basin. (30 hskp)
222. Anjar, Johanna, 2008: A sedimentological and stratigraphical study of Weichselian sediments in the Tvärkroken gravel pit, Idre, west-central Sweden. (30 hskp)
223. Stefanowicz, Sissa, 2008: Palynostratigraphy and palaeoclimatic analysis of the Lower - Middle Jurassic (Pliensbachian - Bathonian) of the Inner Hebrides, NW Scotland. (15 hskp)
224. Holm, Sanna, 2008: Variations in impactor flux to the Moon and Earth after 3.85 Ga. (15 hskp)
225. Bjärnborg, Karolina, 2008: Internal structures in detrital zircons from Hamrånge: a study of cathodoluminescence and back-scattered electron images. (15 hskp)
226. Noresten, Barbro, 2008: A reconstruction of subglacial processes based on a classification of erosional forms at Ramsvikslandet, SW Sweden. (30 hskp)
227. Mehlqvist, Kristina, 2008: En mellanjurassisk flora från Bagå-formationen, Bornholm. (15 hskp)
228. Lindvall, Hanna, 2008: Kortvariga effekter av tefranedfall i lakustrin och terrestrisk miljö. (15 hskp)
229. Löfroth, Elin, 2008: Are solar activity and cosmic rays important factors behind climate change? (15 hskp)
230. Damberg, Lisa, 2008: Pyrit som källa för spårämnen – kalkstenar från övre och

mellersta Danien, Skåne. (15 hskp)

331. Cegrell, Miriam & Mårtensson, Jimmy, 2008: Resistivity and IP measurements at the Bolmen Tunnel and Ådalsbanan, Sweden. (30 hskp)
232. Vang, Ina, 2008: Skarn minerals and geological structures at Kalkheia, Kristiansand, southern Norway. (15 hskp)
233. Arvidsson, Kristina, 2008: Vegetationen i Skandinavien under Eem och Weichsel samt fallstudie i submoräna organiska avlagringar från Nybygget, Småland. (15 hskp)
234. Persson, Jonas, 2008: An environmental magnetic study of a marine sediment core from Disko Bugt, West Greenland: implications for ocean current variability. (30 hskp)
235. Holm, Sanna, 2008: Titanium- and chromium-rich opaque minerals in condensed sediments: chondritic, lunar and terrestrial origins. (30 hskp)
236. Bohlin, Erik & Landen, Ludvig, 2008: Geofysiska mätmetoder för prospektering till ballastmaterial. (30 hskp)
237. Brodén, Olof, 2008: Primär och sekundär migration av hydrokarboner. (15 hskp)
238. Bergman, Bo, 2009: Geofysiska analyser (stångslingram, CVES och IP) av lagerföljd och lakvattenrörelser vid Albäcksdeponin, Trelleborg. (30 hskp)
239. Mehlqvist, Kristina, 2009: The spore record of early land plants from upper Silurian strata in Klinta 1 well, Skåne, Sweden. (45 hskp)
239. Mehlqvist, Kristina, 2009: The spore record of early land plants from upper Silurian strata in Klinta 1 well, Skåne, Sweden. (45 hskp)
240. Bjärnborg, Karolina, 2009: The copper sulphide mineralization of the Zinkgruvan deposit, Bergslagen, Sweden. (45 hskp)
241. Stenberg, Li, 2009: Historiska kartor som hjälp vid jordartsgeologisk kartering – en pilotstudie från Vångs by i Blekinge. (15 hskp)
242. Nilsson, Mimmi, 2009: Robust U-Pb baddeleyite ages of mafic dykes and intrusions in southern West Greenland: constraints on the coherency of crustal blocks of the North Atlantic Craton. (30 hskp)
243. Hult, Elin, 2009: Oligocene to middle Miocene sediments from ODP leg 159, site 959 offshore Ivory Coast, equatorial West Africa. (15 hskp)
244. Olsson, Håkan, 2009: Climate archives and the Late Ordovician Boda Event. (15 hskp)
245. Wollein Waldetoft, Kristofer, 2009: Svekofennisk granit från olika metamorfa miljöer. (15 hskp)
246. Månsby, Urban, 2009: Late Cretaceous coprolites from the Kristianstad Basin, southern Sweden. (15 hskp)
247. MacGimpsey, I., 2008: Petroleum Geology of the Barents Sea. (15 hskp)
248. Jäckel, O., 2009: Comparison between two sediment X-ray Fluorescence records of the Late Holocene from Disko Bugt, West Greenland; Paleoclimatic and methodological implications. (45 hskp)
249. Andersen, Christine, 2009: The mineral composition of the Burkland Cu-sulphide deposit at Zinkgruvan, Sweden – a supplementary study. (15 hskp)
250. Riebe, My, 2009: Spinel group minerals in carbonaceous and ordinary chondrites. (15 hskp)
251. Nilsson, Filip, 2009: Föroreningsspridning och geologi vid Filborna i Helsingborg. (30 hskp)
252. Peetz, Romina, 2009: A geochemical characterization of the lower part of the Miocene shield-building lavas on Gran Canaria. (45 hskp)
253. Maria Åkesson, 2010: Mass movements as contamination carriers in surface water systems – Swedish experiences and risks. (45 hskp)
254. Elin Löfroth, 2010: A Greeland ice core perspective on the dating of the Late Bronze Age Santorini eruption. (45 hskp)

LUNDS UNIVERSITET

Institutionen för geo- och ekosystemvetenskaper
Enheten för geologi
Sölvegatan 12, 223 62 Lund